Dispersion of Very Short Microwave Pulses in Waveguide

M. ITO, MEMBER, IEEE

Abstract—A very short carrier pulse propagating in waveguide is subject to dispersion which causes distortion of both the envelope and the carrier wave of the pulse. The results of a stationary phase analysis of the problem are presented and results of experimental work at *X* band are described.

The spectral separation property of the dispersive line which enables it to operate as an elementary spectrum analyzer are discussed and experimental evidence demonstrating this property is presented.

I. Introduction

DISPERSION in waveguide is of considerable practical importance in the transmission of both FM and AM signals; in some systems it may be the predominant source of distortion. This paper is concerned with the dispersion of AM signals having the form of very short pulses in conventional hollow waveguide.

The most familiar effect associated with dispersion of short carrier pulses in waveguide is stretching or spreading of the pulse envelope. Lesser known is the phenomenon of angle modulation of the carrier wave within the output pulse, which occurs in order to preserve the spectral bandwidth of the input pulse. These phenomena are not always undesirable; pulse compression radar systems, for example, take advantage of these phenomena to reduce peak pulse power.

Exact theoretical analysis of the propagation of pulses in waveguide has not been very productive because of the difficulty in evaluating the contour integral [1], [2] which describes the signal at some distance along the waveguide axis from the source point. This integral has been evaluated exactly in terms of known functions only for an impulse excitation [1], [3]. The convolution integral which describes the response for other excitations is about as difficult to evaluate as the contour integral. Cohn [2] has resorted to numerical integration to calculate the response due to a step-modulated carrier wave. Approximate analyses exist for a number of elementary excitations including 1) a step function [4], 2) a step-modulated carrier wave [1], [5]–[9], 3) a rectangular envelope carrier pulse [10], [11], [12], and 4) a Gaussian envelope carrier pulse [13]. The latter two cases are of interest here but the analyses referred to above, which employ a quadratic approximation to the phase characteristic about a fixed frequency, can only be applied to narrow-band signals.

Past experimental investigations [14]–[20] of the propagation of carrier pulses in waveguide have not demonstrated the severe distortions that dispersion can cause, largely due to the relatively large ratios of pulse length (in free space) to the length of waveguide that were employed. These investigations include experiments with sound pulses [18], [19], [20] transmitted over acoustic waveguide since the propagation function for certain types of acoustic waveguide is similar to that of electromagnetic waveguides. Recent developments in techniques of generating and measuring very short microwave pulses have made it possible to conduct further investigations of the distortions due to dispersion. The results of some work with fractional-nanosecond *X*-band pulses are described here. The observed results can largely be explained by means of a simple approximate analysis.

II. Nature of the Output Pulse

An homogeneous hollow waveguide of constant cross section which has perfectly conducting walls and which is excited in only one of its modes has a propagation function of the form

$$\beta(\omega) = -\omega T\sqrt{1-(\omega_c/\omega)^2} \tag{1}$$

where

$$\omega_c = 2\pi f_c \quad (f_c = \text{modal cutoff frequency})$$

$$T = \text{free space propagation time.}$$

The function $\beta(\omega)$ gives the total phase shift (in radians) of a steady-state signal of radian frequency ω propagating through the waveguide.

If the waveguide is excited in a single mode by an input signal $x(t)$ with Fourier transform $X(\omega)$, the output response from the waveguide can be described by the Fourier integral

$$y(t) = \frac{1}{2\pi}\int_{-\infty}^{\infty} X(\omega)e^{j[\omega t+\beta(\omega)]}d\omega. \tag{2}$$

Under certain conditions to be briefly discussed later, a simple asymptotic evaluation of (2) can be obtained by applying Kelvin's principle of stationary phase.[1]

For the integrand of (2), the points of stationary phase are the solutions of the equation

$$t = -\frac{d\beta(\omega)}{d\omega} \equiv -\beta'(\omega). \tag{3}$$

The function $\beta'(\omega)$ is usually called the group-delay function. According to the stationary phase principle, the response at a time $t=\tau$ can be interpreted as being

Manuscript received September 17, 1964; revised February 1, 1965.

The author is with the Radio and Electrical Engineering Div., National Research Council, Ottawa, Canada.

[1] See, for example, Papoulis [22].

built up largely from a band of spectral components that have a group delay nearly equal to τ. The solution of (3) for positive ω is given by

$$\omega_s = \frac{\omega_c t/T}{\sqrt{(t/T)^2 - 1}} \qquad t > T. \tag{4}$$

Except for sign, the solution for negative ω is identical to the above. Figure 1 shows a plot of the function

$$\frac{\omega}{\omega_c} = \frac{t/T}{\sqrt{(t/T)^2 - 1}}.$$

This curve describes the group-delay characteristic of the waveguide and gives the location of the points of stationary phase as a function of time.

The stationary phase approximation to $y(t)$ is given by

$$y_1(t) = \sqrt{\frac{2}{\pi \left| \beta''(\omega_s) \right|}} \left| X(\omega_s) \right| \cos\left[\omega_s t + \beta(\omega_s) + \frac{\pi}{4}\right] \qquad t > T \tag{5}$$

which, for a given $X(\omega)$, best applies for large t and T. This approximation assumes any nonlinear variations of the phase of $X(\omega)$ to be small compared to the nonlinear variation of $\beta(\omega)$. Otherwise, it is necessary to include a small additional term in the argument of the cosine function in (5).

The conditions under which stationary phase analysis can be applied are difficult to specify quantitatively since the analysis yields no estimate of the error in the end result. Qualitatively, however, the requirements in the present case are 1) that the dispersion be large, that is, $d^2\beta/d\omega^2 \equiv \beta''(\omega)$ be large for all ω_s values of interest, and 2) that the input spectrum be wide band because the analysis does not take into account the variation of $X(\omega)$ in the region about the point of stationary phase.

The error in $y_1(t)$ due to small dispersion is greatest for values of t close to T or equivalently for ω_s values much greater than ω_c. Examination of the response due to an impulse excitation, which is free of errors due to variations in $X(\omega)$, enables one to estimate a lower bound on the values of t for which $y_1(t)$ is a good approximation to $y(t)$. For an impulse excitation the error in the envelope of $y_1(t)$ is less than 1 per cent for values of t greater than the value t_a given by

$$t_a = T\sqrt{1 + (15/\omega_c T)^2}. \tag{6}$$

That is, the analysis begins to fail for stationary phase points above the point ω_a, given by

$$\omega_a = \omega_c\sqrt{1 + (\omega_c T/15)^2}. \tag{7}$$

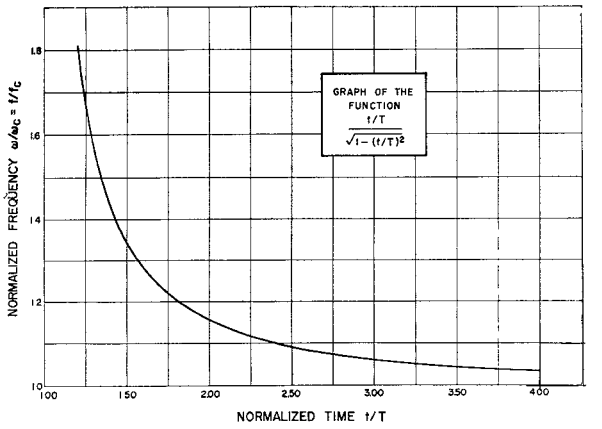

Fig. 1. Universal curve giving: 1) the location of the stationary phase point as a function of time, 2) group-delay characteristics of the waveguide, and 3) instantaneous carrier frequency within the dispersed pulse.

By applying the convolution theorem, it may be argued that t_a is a lower bound on t for other excitations. It follows that ω_a is an upper bound on ω_s. For the experiments to be described later, ω_a is very much larger than the highest ω_s values of interest because of the largeness of the product $\omega_c T$ and the location of the signal spectrum. Consequently, the error in $y_1(t)$ due to small dispersion is considered to be small.

The error in $y_1(t)$ due to moderate variation of $X(\omega)$ in the region of the stationary phase point can be investigated by employing the more general saddle-point method of integration [1], [21], [23]. This method of integration shows that $y_1(t)$ is the first-order term of a series involving $X(\omega)$ and the derivatives of $X(\omega)$, all evaluated at $\omega = \omega_s$. Haggarty [23] shows that the percentage error ϵ that results from neglecting the higher order terms in the series is less than or equal to an upper bound ϵ_b, given by

$$\epsilon_b = \left| \frac{50X''(\omega)}{\beta''(\omega)X(\omega)} \right|_{\omega=\omega_s}. \tag{8}$$

The bound ϵ_b tends to be less for a wide-band signal than a narrow-band signal of similar shape because the factor $\left| X''(\omega_s)/X(\omega_s) \right|$ is generally smaller for the wide-band case. However, even for relatively narrow-band signals, the error bound will be small if the values of $\left|\beta''(\omega_s)\right|$ over the signal bandwidth are very large. For the experiments described in this paper, the bandwidths of the input signals and the strength of the dispersion are such as to make this source of error small.

The simple expression for the output response that results from stationary phase analysis has several interesting properties. To facilitate the discussion, $y_1(t)$ is separated into two factors: 1) an envelope function proportional to $\left|X(\omega_s)\right| / \sqrt{\left|\beta''(\omega_s)\right|}$, and 2) a gliding tone described by $\cos\left[\omega_s t + \beta(\omega_s) + \pi/4\right]$.

First, consider the nature of the gliding tone or swept-frequency carrier wave. If the "instantaneous carrier frequency" f_i within the dispersed pulse is defined to be $f_i=(1/2\pi)(d[\omega_s t+\beta(\omega_s)]/dt)$, it may easily be shown that the time variation of f_i is given by the relationship $f_i(t)/f_c=\omega_s(t)/\omega_c$. That is, the instantaneous carrier frequency at a time $t=\tau$ is equal to the frequency for which the group delay through the waveguide is equal to τ. The rate of frequency sweep df_i/dt is not a linear function of time, and it is evident that the nature of the frequency sweep is essentially a property of the waveguide rather than of the input signal. The input signal affects only the shape of the output envelope and its time position relative to the gliding tone. For example, if the input signal is a carrier pulse with carrier frequency f_0, there is a definite relationship between the time position of the output envelope and the time that the instantaneous carrier frequency passes through the value f_0. For the purpose of demodulation, the output carrier wave can be said to be swept in frequency about $f=f_0$.

Next, consider the envelope of the output pulse which we have seen is proportional to $|X(\omega_s)|/\sqrt{|\beta''(\omega_s)|}$. For a carrier pulse input excitation, $X(\omega)$ as a function of ω is symmetrical about the input carrier frequency. However, because of the nonlinear relationship between ω_s and t and because of the attenuation factor $1/\sqrt{|\beta''(\omega_s)|}$, the output envelope as a function of time is not symmetrical about any instant of time. Qualitatively, the envelope may be described as having a sharp attack and slow decay. Nevertheless, the output envelope is closely related to the shape of input spectrum. Anderson and Barnes [18], for example, have recognized the spectral separation properties of a dispersive acoustic waveguide in attempting to calculate the spectrum of an acoustic pulse, but the intuitive argument employed does not take into account the dispersive attenuation factor $1/\sqrt{|\beta''(\omega_s)|}$. Tverskoi [24], among others, has also suggested using a dispersive line for spectrum analysis.

The time dependence of the dispersive attenuation factor accounts for changes in the degree of dispersion across the frequency spectrum of the input signal. A band of spectral components subject to strong dispersion becomes spread over a longer time interval than a band of spectral components of the same bandwidth and of the same energy content that is not as strongly dispersed. It follows then that the peak amplitude of the response in the low dispersion case must necessarily be larger than in the high dispersion case. This is, of course, a fundamental concept in "chirp" radar systems.

Figure 2 shows plots of $\sqrt{T/\omega_c}/\sqrt{|\beta''(2\pi f)|}$ vs. f/f_c and t/T. With the aid of Fig. 2 and Fig. 1, the output pulse envelope can be cacullated from a knowledge of the input pulse spectrum, and vice versa. An application of the former process is illustrated diagrammatically in Fig. 13.

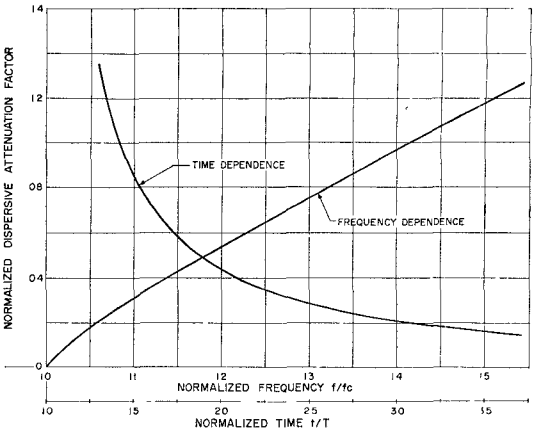

Fig. 2. Frequency and time dependence of the dispersive attenuation factor.

III. Experimental Results

The experimental work described here was carried out at X band and consisted of two different experiments. In the first experiment synchronous detection was employed in order to obtain resolution of the angle modulation structure within the dispersed pulse; while in the second experiment, in which much shorter pulses were used, nonsynchronous detection was employed as a means of demonstrating the spectral separation properties of the dispersive transmission line. In order to keep losses low, but more important, in order to keep differential attenuation across the frequency band of interest small, a comparatively short length of RG/52 waveguide (about 100 cutoff wavelengths long) was used in both experiments. This waveguide was excited in the dominant TE_{10} mode, which has a cutoff frequency of 6.56 Gc/s. In both cases, heterodyne detection was employed because the dispersed pulses could not be directly observed.

A. The First Experiment

A block diagram of the first experimental setup is shown in Fig. 3. The diode modulator, which incorporates a crystal diode mounted across the waveguide, produces short carrier pulses of about 0.9 ns half-amplitude width and variable carrier frequency. These pulses have an envelope that is approximately Gaussian in shape.

The dispersed pulses at the output of the test waveguide section are observed with a receiver comprised of a wide-band multiplier (an untuned crystal mixer), a low-pass filter, and a sampling oscilloscope. Corresponding to a dispersed pulse represented by

$$a(t)\cos[2\pi f_0 t+\phi(t)+\phi_0] \tag{9}$$

where $a(t)$ is the envelope, $\phi(t)$ is an angle modulation function, and ϕ_0 is a phase constant, the output of the receiver is proportional to

$$a(t)\cos[\phi(t)+(\phi_0-\phi_{LO})] \tag{10}$$

where ϕ_{LO} is the LO phase. Because of the synchronous detection scheme, the angle modulation function $\phi(t)$ and the phase difference $(\phi_0-\phi_{LO})$ remain the same from pulse to pulse. Consequently, with the recurrent display scheme employed, a stationary waveform is observed. From this waveform the envelope function $a(t)$ can be determined and the angle modulation structure $\phi(t)$ or the FM structure $(1/2\pi)$ $(d\phi/dt)$ can be examined. A phase shifter in the LO signal path allows adjustment of the phase difference $(\phi_0-\phi_{LO})$ to any desired value.

Figure 4 shows oscillograms of detected pulses with and without the test waveguide section in the system. Unsymmetrical output envelopes having a sharp attack and slow decay are observed to result from more or less symmetrical input envelopes. As expected, the amount of envelope stretching is seen to increase as the carrier frequency of the input pulses approaches the waveguide cutoff frequency.

The envelope of the pulses generated by the modulator were found to be well approximated by a Gaussian function matched at the half-amplitude points (Fig. 5), and this function was employed in calculating the envelope of the dispersed pulses emerging from the waveguide. Calculated output waveforms, determined from the stationary phase formula, are shown in Fig. 6 for input carrier frequencies equal to 7.60 Gc/s and 7.86 Gc/s. Experimentally measured output envelope points corresponding to the peaks of the beat structure are also shown in Fig. 6. The experimental points agree reasonably well with the calculated envelopes except in the vicinity of $t/T=2.25$ where the measured points dip significantly below the calculated envelopes. Since the discrepancy occurs in the vicinity of the same value of t/T in both cases, it is attributed to a dip in the steady-state system response in the vicinity of 7.30 Gc/s, which is the frequency for which the normalized group delay is about 2.25. Such a dip has been experimentally confirmed.

Measurement of the angle modulation function $\phi(t)$ was carried out as follows. By adjusting the phase shifter in the LO signal path, a notch was produced in the wide central lobe that appears in the detected output pulses shown in Fig. 4. Because points on the angle modulation curve are most easily determined from a measurement of zero crossings, the bottom of this notch was brought down to the axis of zero crossings for this purpose. Figure 7 shows the resultant oscillogram for the case $f_0=7.60$ Gc/s. This means that the argument of the cosine function in expression (10), namely,

$$\phi(t)+(\phi_0-\phi_{LO})\equiv W(t) \tag{11}$$

has the principal value $\pm(\pi/2)$ at the time corresponding to the notch. Consequently, measurement of the times of zero crossings relative to this notch gives the times when $W(t)$ differs from $\pm(\pi/2)$ by an integral multiple of π.

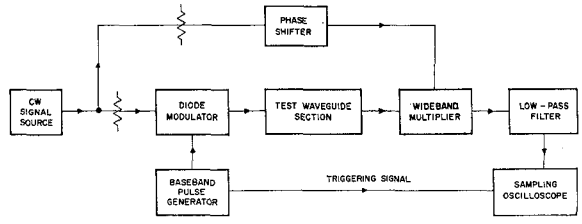

Fig. 3. Basic block diagram of the first experimental setup.

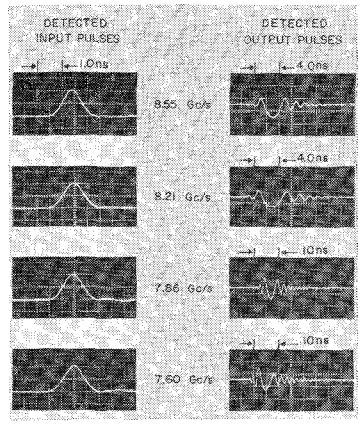

Fig. 4. Synchronously detected input and output pulses for various carrier frequencies.

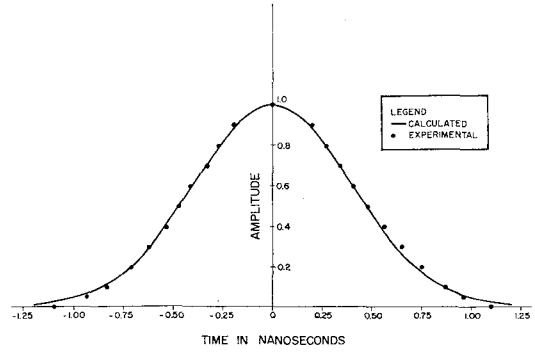

Fig. 5. Measured input pulse envelope for a carrier frequency of 7.60 Gc/s and a Gaussian approximation to this envelope.

Figure 8 shows measured values of the angle modulation function $W(t)$ for the cases $f_0=7.60$ Gc/s and $f_0=7.86$ Gc/s. Also shown are the theoretical angle modulation functions calculated from the stationary phase formula

$$W_1(t)=\omega_c T\sqrt{(t/T)^2-1}-2\pi f_0 t-\phi_1 \tag{12}$$

where ϕ_1 is a constant chosen to bring the calculated curve into vertical coincidence with the measured curve at the notch point. The agreement between theoretical and experimental curves is remarkably good. It is evident that the slope of the angle modulation curve, which is proportional to the FM characteristic, is not a linear function of time.

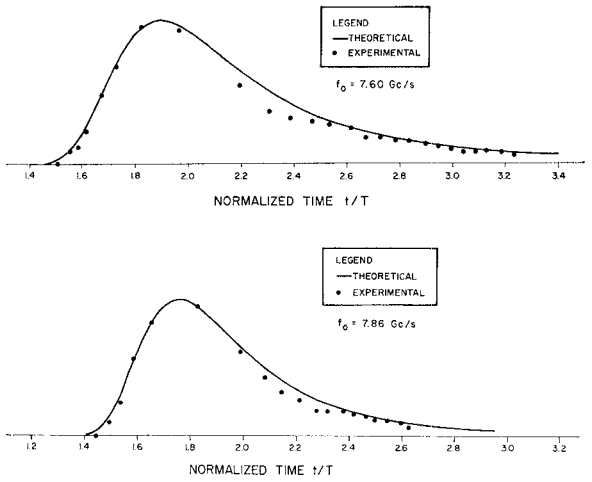

Fig. 6. Measured and calculated envelopes of dispersed output pulses.

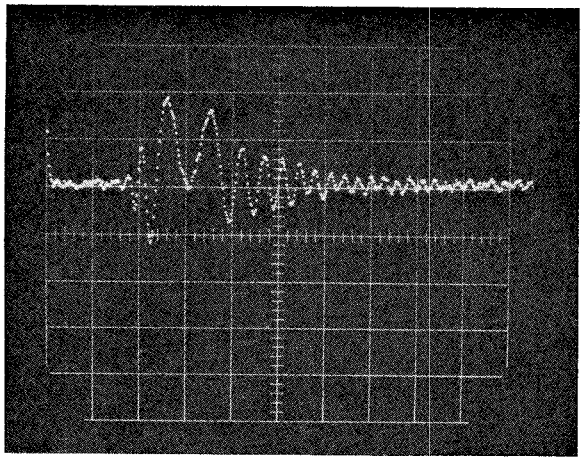

Fig. 7. Typical waveform used in measuring the angle modulation function. Time scale is 5.0 ns/major div. $f_0 = 7.60$ Gc/s.

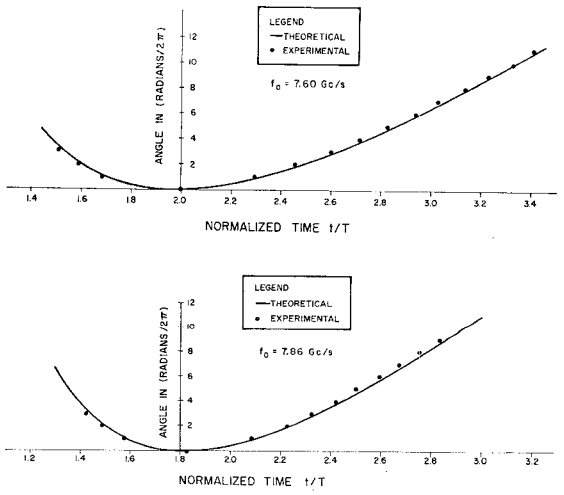

Fig. 8. Measured and calculated angle modulation functions for the dispersed output pulses shown in Fig. 6.

B. The Second Experiment

A block diagram of the second experimental setup is shown in Fig. 9. The input carrier pulses to the waveguide are generated by exciting the waveguide with band-limited impulses produced by a microwave "noise" generator of the impulse type [25]. The output amplitude spectrum of this "noise" generator is uniform within a half dB from 10 Mc/s well up into *X* band. The waveguide acts as a high-pass filter, thereby creating a band-pass spectrum with a 6 dB-bandwidth of about 5.0 Gc/s. The nominal carrier frequency of the pulses generated is about 9.0 Gc/s, and the half-amplitude width of these pulses is estimated to be about 0.2 ns. Measurement of this pulse width was not feasible because of bandwidth limitations of the detector output circuit and the oscilloscope.

The receiver in this experiment is similar to the one previously used except that the *LO* frequency is generally not coincident with the carrier frequency of the input pulses; nor is the *LO* phase locked to that of the input pulses. The receiver functions basically as a fixed bandwidth, band-pass filter whose center frequency is equal to the *LO* frequency. The receiver bandwidth is governed by the low-pass filter on the output of the multiplier.

Figure 10 shows oscillograms of observed receiver outputs for a number of *LO* frequencies and with a low-pass filter bandwidth (6 dB) of 1.1 Gc/s. The time base is triggered by the envelope of the input pulses to the waveguide. The somewhat unusual display results from sampling of an oscillatory waveform whose phase changes more or less randomly from pulse to pulse, relative to an invariant envelope. Since the phase can be presumed to go through all possible values, the envelope of the dot pattern is the envelope of the oscillatory waveform.

Figure 11 shows similar oscillograms taken with a low-pass filter bandwidth of 0.20 Gc/s. For these oscillograms the mixer was intentionally operated with a low *LO* level so that a significant part of the output is due to direct detection of the pulse envelope. The resultant oscillograms clearly demonstrate movement of the dot pattern along the detected envelope.

The previously mentioned oscillograms can be interpreted from either of two asymptotically equivalent viewpoints: 1) in terms of a gliding tone, and 2) in terms of group delay of spectral components; both of these viewpoints are discussed in Section III-B, 1) and Section III-B, 2).

1) *Gliding Tone Interpretation:* According to the stationary phase analysis, the output signal from the waveguide will have the form of a swept-frequency carrier wave of finite duration. On this basis it can be shown that the overall behavior of the system is much like that of a conventional panoramic spectrum analyzer acting on a CW signal. The roles of the local oscillator and the input signal are interchanged but the interpretation of

the end results is similar. The use of a zero intermediate frequency (IF) eliminates the usual "image" problem. As with the panoramic analyzer, the displayed (IF) pulse width is governed by the sweep rate of the heterodyned signal across the IF pass band and by the IF bandwidth. When the gliding tone sweeps through the receiver pass band in a time comparable to or shorter than the width of the receiver impulse response, the receiver output begins to resemble the impulse response. However, when the frequency scan is slow, the ratio of output amplitude to input amplitude traces out the receiver pass band. Conversely, the width of the receiver time response gives an indication of the sweep rate. In Fig. 10, for example, it is observed that the dot pattern decreases in width as the *LO* frequency is increased. This indicates that the sweep rate is increasing as the instantaneous carrier frequency increases, which is in agreement with the stationary phase prediction. In Fig. 11, it is observed that the IF pulse more or less reaches its limiting width within the range of *LO* frequencies shown.

For a fixed *LO* frequency but variable IF bandwidth on the other hand, the IF pulse width tends to decrease with decreasing IF bandwidth up to a certain point and then begins to increase. For example, consider two specific *LO* frequencies, $f_{LO}=11.09$ Gc/s, and $f_{LO}=7.64$ Gc/s, in Figs. 10 and 11. For the case $f_{LO}=11.09$ Gc/s it is observed that decreasing the IF bandwidth causes the IF pulse width to increase whereas, for the case $f_{LO}=7.64$ Gc/s, decreasing the IF bandwidth causes the IF pulse width to decrease.

The time at which the gliding tone sweeps through the *LO* frequency can be estimated from the time position of the peak receiver output. For a rapidly sweeping carrier wave, the peak receiver output occurs at approximately a constant time delay after the instantaneous carrier frequency sweeps through the *LO* frequency. For a slow sweep, however, the amplitude variation of the gliding tone must be taken into account. In the present case, the amplitude of the tone decreases with decreasing instantaneous carrier frequency for most of the frequency sweep because of the effect of the dispersive attenuation factor. This causes the peak receiver output to occur somewhat earlier than expected. Compare Figs. 10 and 11, for example. Taking the location of the peak for $f_{LO}=11.09$ Gc/s as time reference, one observes that for a *LO* frequency of say $f_{LO}=7.64$ Gc/s, the pulse peak occurs earlier in Fig. 10, where a wide bandwidth low-pass filter was used, than in Fig. 11, where a narrower bandwidth low-pass filter was employed.

Figure 12 shows a plot of *LO* frequency vs. time position of the peak receiver output, measured relative to the position of the pulse peak for an *LO* frequency equal to 10.64 Gc/s. These measurements were made from oscillograms similar to those of Fig. 11 but in which the direct detection component was suppressed. Precise time delay between the input pulse to the waveguide and the output pulse from the receiver was not measured; and

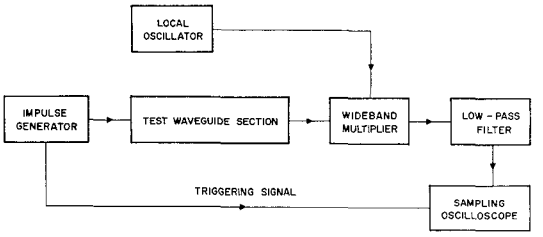

Fig. 9. Basic block diagram of the second experimental setup.

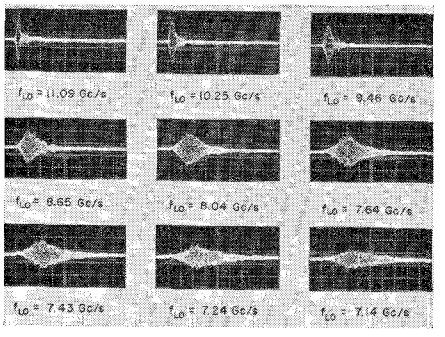

Fig. 10. Receiver output for various *LO* frequencies. Low-pass filter bandwidth = 1.1 Gc/s. The time scale is 5.0 ns/major div. Time increases from left to right and the triggering instant is fixed relative to the vertical grid lines for all oscillograms.

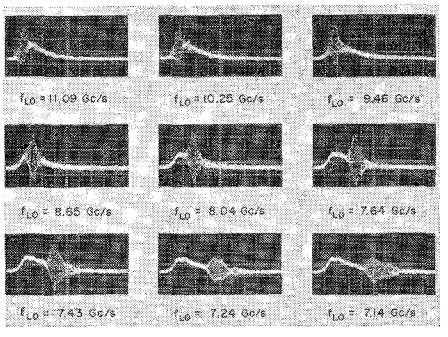

Fig. 11. Oscillograms similar to those of Fig. 10 but with a low-pass filter bandwidth of 0.20 Gc/s. A significant part of the receiver output is due to direct detection of the envelope of the dispersed pulse.

in order to make a comparison with the theoretical curve, the horizontal position of the measured points on the graph was fixed by placing the point corresponding to an *LO* frequency of 10.64 Gc/s on the theoretical curve. With this horizontal placement of the measured points, it is seen that they fit the theoretical curve fairly well down to about $f=7.4$ Gc/s, after which the measured points begin to appear somewhat earlier than the theoretical prediction. Some of this discrepancy may be attributed to uncertainty in locating the pulse peak; but it is largely attributed to a slow frequency sweep rate, the effect of which has been previously discussed. A slow sweep rate is indicated by the increasing width of the receiver output which is quite noticeable for *LO* frequencies below about 7.6 Gc/s.

2) *The Spectral Separation Viewpoint:* Stationary phase theory indicates that a spectral component of the

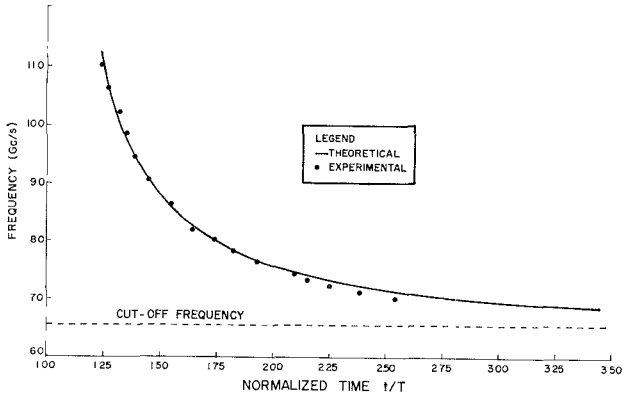

Fig. 12. Plot of the relative time positions of the peak receiver output as the *LO* frequency is varied. Receiver bandwidth = 0.40 Gc/s. The theoretical curve in the group-delay characteristic of the RG/52 waveguide.

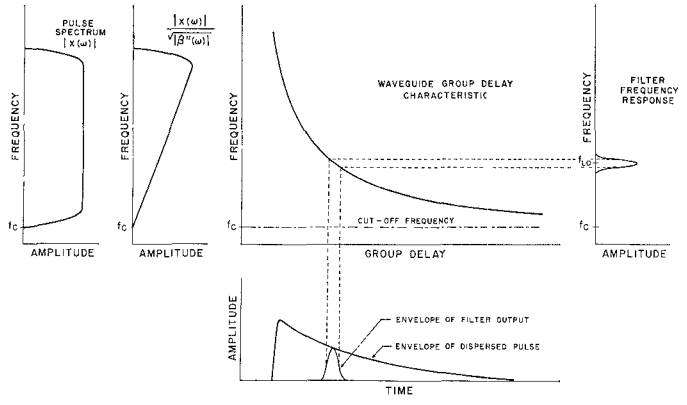

Fig. 13. Spectral separation process in a strongly dispersive system.

input signal at a given frequency contributes most to the output signal from the transmission system in the vicinity of a time equal to the group-delay time of that component through the system. For waveguide, the frequency vs. group-delay characteristic is a monotonically decreasing function of increasing group delay. Consequently, the theory suggests that contiguous bands of spectral components of the output signal will be separated in time in an orderly way. This in turn suggests that a frequency selective (band-pass) filter can be used to separate the parts of the response due to different frequency bands of the input signal. This spectral separation process is indicated diagrammatically in Fig. 13.

If the spread of group delays for the spectral components falling within the filter bandwidth is large compared to the filter impulse response width, then the stationary phase analysis can be reapplied. That is, the filter output is essentially described by (5) modified by the multiplicative factor $|H(\omega_s)|$, where $H(\omega)$ is the filter transfer function. This means that the time spread of the filter output response is essentially the spread of group-delay times of the spectral components falling within the filter bandwidth. This, in turn, accounts for the increasing width of the time responses that occurs in Fig. 10 as the center frequency of the analyzing filter (i.e., the *LO* frequency) is lowered toward the cutoff frequency.

As the spread of group-delay times becomes shorter than that previously described, the filter begins to treat the input excitation as an impulse. This explains the more or less constant response widths observed in Fig. 11.

It is evident from the previous discussion that the time position of the peak filter output gives a measure of the average group delay of the spectral components falling within the filter pass band. In fact, for a first-order estimate, one can equate the time position of the peak, corrected for a fixed time delay due to the analyzing filter, with the group delay of the spectral component at the center frequency of the filter. A better estimate is obtained if one takes into account the effect of the dispersive attenuation factor in displacing the peak response forward in time from the group-delay time of the central spectral component, or if one employs a filter with a bandwidth narrow enough to overshadow the effect of the dispersive attenuation factor. This latter principle was employed in plotting Fig. 12, which can be considered to be a calibration of the group-delay characteristic of the waveguide.

From either of the foregoing viewpoints, it is seen that the dispersive properties of the waveguide enable it to function as a crude form of spectrum analyzer. In the present work we have experimentally calibrated the nonlinear frequency vs. time scale and have studied the effect of different post-detector bandwidths on the operation of the system.

IV. Conclusions

The main conclusions to be drawn from the analysis and experimental work described in this paper are:

1) Strong dispersion in waveguide causes both the envelope and carrier wave of a short carrier pulse to become severely distorted.

2) The carrier wave becomes distorted into a gliding tone which sweeps through the input carrier frequency. The frequency sweep of this tone, which is nonlinear with time, is essentially independent of the input pulse shape.

3) The envelope of the output pulse is asymmetrical, but is closely related to the spectrum of the input signal.

4) The degree of the foregoing distortions increases with a) decreasing width of the input pulses, b) decreasing carrier frequency, and c) increasing length of waveguide.

5) The waveguide, combined with an appropriate receiver, can be made to operate as a spectrum analyzer.

V. Acknowledgment

The author is grateful to his colleagues at the National Research Council of Canada, in particular to J. K. Pulfer, for helpful advice and criticism given in the course of preparing this paper.

References

[1] Cerrillo, M. V., Transient phenomena in waveguides, Tech Rept 33, MIT Research Lab. of Electronics, Cambridge, Mass., Jan 1948.
[2] Cohn, G. I., Electromagnetic transients in waveguide, *Proc. NEC*, vol 8, Oct 1952, pp 284–295.
[3] Cotte, M., Propagation d'une Perturbation dans un Guide Electrique, *Ann. Télécommun*, vol 1, Mar–Apr 1946, pp 49–52.
[4] ——, Propagation d'une Impulsion sur un Guide D'Ondes, *Onde elect.*, vol 34, Feb 1954, pp 143–146.
[5] Pearson, J. D., The transient motion of sound waves in tubes, *Quart. J. Mech. and Appl. Math.*, vol 6, pt 3, 1953, pp 313–335.
[6] Poincelot, P., Propagation d'un Signal Le Long d'un Guide D'Ondes, *Ann. Télécommun.*, vol 9, Nov 1954, pp 315–317.
[7] Karbowiak, A. E., Propagation of transients in waveguides, *Proc. IEE (London)*, vol 104, pt C, Sep 1957, pp 339–348.
[8] Kovtun, A. A., Transient processes in waveguide, *Radio Eng. Electron.*, vol 3, no. 5, 1958, pp 103–122.
[9] Gajewski, R., Influence of wall losses on pulse propagation in waveguides, *J. Appl. Phys.*, vol 29, Jan 1958, pp 22–24.
[10] Elliot, R. S., Pulse waveform degradation due to dispersion in waveguide, *IRE Trans. on Microwave Theory and Techniques*, vol MTT-5, Oct 1957, pp 254–257.
[11] Knop, C. M., and G. I. Cohn, Comments on "pulse waveform degradation due to dispersion in waveguide," *IEEE Trans. on Microwave Theory and Techniques (Correspondence)*, vol MTT-11, Sep 1963, pp 445–447.
[12] Wanselow, R. D., Rectangular pulse distortion due to a nonlinear complex transmission propagation constant, *J. Franklin Inst.*, vol 274, Sep 1962, pp 178–184.
[13] Forrer, M. P., Analysis of millimicrosecond RF pulse transmission, *Proc. IRE*, vol 46, Nov 1958, pp 1830–1835.
[14] Winter, D. F., E. A. Guillemin, L. J. Chu, and M. V. Cerrillo, Transient phenomena in waveguides, Quart. Prog. Rept, MIT Research Lab. of Electronics, Cambridge, Mass., Apr 1947.
[15] Beck, A. C., Microwave testing with millimicrosecond pulses, *IRE Trans. on Microwave Theory and Techniques*, vol MTT-2, Apr 1954, pp 93–99.
[16] ——, Measurement techniques for multimode waveguides, *IRE Trans. on Microwave Theory and Techniques*, vol MTT-3, Apr 1955, pp 35–41.
[17] Saxton, W. A., and H. J. Schmitt, Transients in large waveguide, *Proc. IEEE (Correspondence)*, vol 51, Feb 1963, pp 405–406.
[18] Anderson, D. V., and C. Barnes, The dispersion of a pulse propagated through a cylindrical tube, *J. Acoust. Soc. Am.*, vol 25, May 1953, pp 525–528.
[19] Proud, J. M., P. Tamarkin, and E. T. Kornhauser, Propagation of sound pulses in a dispersive medium, *J. Acoust. Soc. Am.*, vol 28, Jan 1956, pp 80–85.
[20] Walther, K., Pulse compression in acoustic waveguide, *J. Acoust. Soc. Am.*, vol 33, May 1961, pp 681–686.
[21] De Bruijn, N. C., *Asymptotic Methods in Analysis*. Amsterdam, Holland: North-Holland Publishing Co., 1958, ch 5.
[22] Papoulis, A., *The Fourier Integral and Its Applications*. New York: McGraw-Hill, 1962, sec 7-7.
[23] Haggarty, R. D., A method of signal design employing saddle-point integration, Rept 41G0009, MIT Lincoln Lab., Lexington, Mass., May 1961.
[24] Tverskoi, V. I., Use of delay system with dispersion of phase velocity for the analysis of spectra of individual radio signals, *Radio Eng. Electron.*, vol 4, no 9, 1959, pp 242–246.
[25] Wind, M., and H. Rapaport, *Handbook of Microwave Measurements*, vols I and II. Brooklyn, N. Y.: Polytech. Inst. Brooklyn Microwave Res. Inst., 1954–1955, sec 14.

The Solution of Guided Waves in Inhomogeneous Anisotropic Media by Perturbation and Variational Methods

G. J. GABRIEL, STUDENT MEMBER, IEEE, AND M. E. BRODWIN, MEMBER, IEEE

Abstract—**The Schroedinger perturbation theory is extended to the boundary value problems of guided electromagnetic waves in cylindrical structures containing inhomogeneous, anisotropic, dissipative media. A general variational principle, which reduces to existing restricted forms valid for nondissipative media, is also formulated. These approximation methods evolve in a unified manner from the eigenvalue formulation of Maxwell's equations wherein the wave numbers are the eigenvalues of a linear operator. The properties of the media are restricted only by the requirement that they be independent of the axial coordinate. Perturbation of the backward wave is considered and the condition for nonreciprocal waveguides is stated. Modification of the perturbation method for application to gyrotropic media is outlined and it is indicated that convergence of the perturbation terms is improved in those media, such as the plasma and semiconductor, which permit a Taylor expansion of the susceptibility tensor in powers of the external field. Two specific examples, whose exact solutions are known, are included to illustrate the application.**

Manuscript received October 23, 1964; revised February 4, 1965. This work was supported by the Advanced Research Projects Agency through the Northwestern University Materials Research Center.

The authors are with the Dept. of Electrical Engineering, Northwestern University, Evanston, Ill.

I. Introduction

THE PROPAGATION of guided electromagnetic waves in cylindrical structures containing anisotropic, inhomogeneous media poses formidable boundary value problems, even under simplifying conditions. In recent years, materials which display induced anisotropy, namely the gyrotropic media, have received considerable attention. Because of the special form of the susceptibility tensors of gyrotropic media, when the external magnetic field is oriented along one of the co-